MECHANISM OF SEISMIC EVENTS AND MECHANICS OF ROCKBURST DAMAGE LABORATORY STUDIES, VISUAL AND SEISMIC OBSERVATIONS

RELATING TILT MEASUREMENTS RECORDED AT MPONENG GOLD MINE, SOUTH AFRICA, TO THE RUPTURE OF AN M 2.2 EVENT

P. Share[1,2], A. Milev[1,2], R. Durrheim[1,2,3], J. Kuijpers[1,2], H. Ogasawara[1,4]
[1]JST-JICA, Science and Technology Research Partnership for Sustainable Development (SATREPS),
[2]Council for Scientific and Industrial Research, South Africa,
[3]University of the Witwatersrand, South Africa,
[4]Ritsumeikan University, Japan

High resolution tiltmeters were installed during 2007 at Mponeng gold mine, South Africa, in an attempt to study and understand the risks posed by in-mine seismic events and to subsequently use the knowledge gained to mitigate the said risks. In December 2007, an M 2.2 event occurred at Mponeng and was detected by the tiltmeters installed. The tilt expected for the M 2.2 event is modelled through the use of numerical and analytical tools and utilizing, as input parameters, characteristics of the event such as the rupture area, the amount of slip, elastic properties of the rock, the state of stress before the event occurred and frictional parameters of the rupture. The calculated tilt values are correlated and compared with the recorded data, and are found to be of the same order. Certain input parameters, such as the initial rupture point, are further constrained by varying them, during modelling, until the calculated and observed tilt values are approximately equal. From modelling, it can be concluded that the rupture point had to be closer to the location of the tiltmeters. In addition, possible locations acting as source areas for the observed aftertilt are determined. These conclusions aside, further modelling needs to be done to quantify the effects of the tunnel close to the tiltmeters and plastic deformation of the rockmass.

INTRODUCTION

High-resolution Tilt Measurements at Mponeng Gold Mine

Rockbursts and similar seismic hazards in deep-level mining are among the most unpredictable yet devastating risks hampering mining production in present times. In an attempt to minimize the rockburst threat various measures have been implemented including rockburst-resistant support and designing mine layouts in an attempt to reduce the amount of seismicity (Spottiswoode and Milev[2006]). In addition, sensitive seismic instruments, such as tiltmeters, have also in some cases been installed in order to study and further understand the risks involved with in-mine seismic events (Spottiswoode and Milev[2006], McGarr and Green[1975]). One such an example was the installation of two tiltmeters at Mponeng gold mine (Figure 1, Ogasawara *et al.*[2009]) in 2007. The site was located at a depth of ~3270 m in a dip pillar, 90 m below the reef which was actively being mined. The high-resolution tiltmeters at Mponeng gold mine were installed close to a large dyke, termed the Pink and Green (PG) dyke (Figure 2). In the vicinity of the tiltmeters, 8 acoustic emission (AE) sensors were also installed (Figure 2a).

TILTMETER INSTALLATION AND DATA

Installation and Data Acquisition

The two tiltmeters (Figure 2b) installed at level 116 of Mponeng gold mine were platform-type with 0.1 μradian sensitivity and 800 μradian recording range. The tiltmeters were installed on specially built piers coupled to the bedrock, which was exposed by removing 1 m of fractured material from the footwall. Tilt was recorded in two ways:

1) Dynamic tilt, where recording commences only when seismically triggered. The recording window for dynamic tilt was approximately two seconds.

2) Quasi-static tilt, where measurements were taken continuously at one minute intervals and stored in memory.

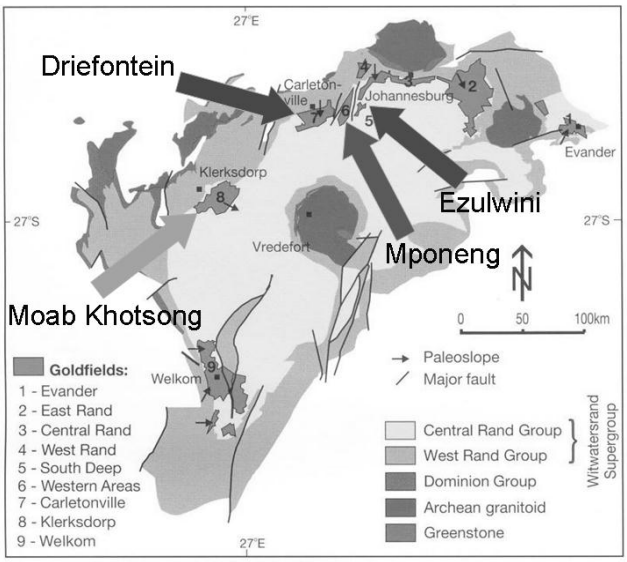

Figure 1. Geology of the Witwatersrand basin, which hosts most of South Africa's gold, and the location of the Mponeneg gold mine relative to three mines where similar research activities have recently been launched

Each tiltmeter measures tilt in two perpendicular directions (x and y, both horizontal). Tilt polarities and magnitudes observed in the perpendicular components

facilitates in determining the direction and amount of maximum tilt (Figure 3).

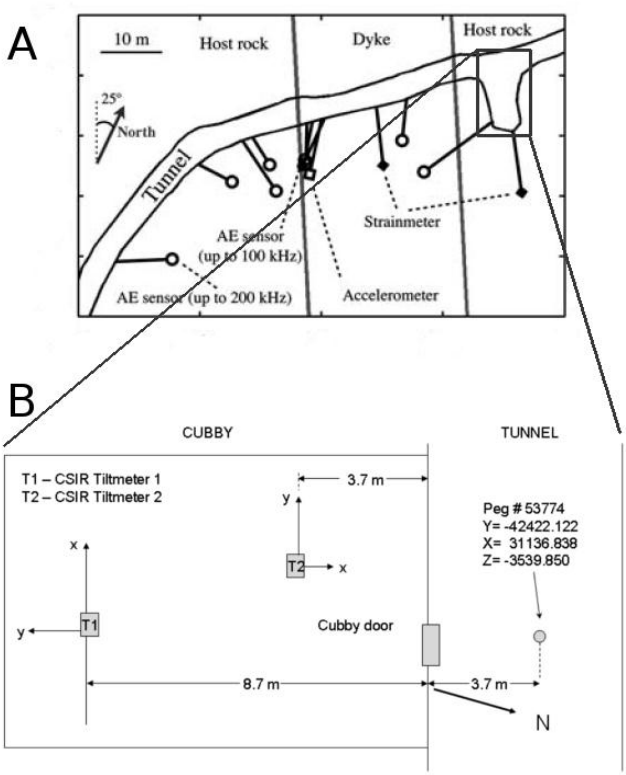

Figure 2. A plan of Mponeng mine level 116 cross-cut 45, showing the installation site and the AE network relative to the Pink and Green dyke (A), and the cubby wherein the tiltmeters were installed (B) (modified from Naoi *et al.*[2011])

A positive tilt change measured in the y-direction relates to an anti-clockwise rotation of the rockmass when the observational direction is +x. In contrast, a positive tilt change as recorded by the x-component is equivalent to a clockwise rotation in the rockmass when viewed in the +y direction (Figure 3). Data acquisition started June 2007 and ended January 2009 during which time a size $M = 2.2$ event occurred on 27 December 2007. Tilt measurements associated with the $M = 2.2$ event are shown in Figure 4. Only tiltmeter 1's values are shown, because during the event tiltmeter 2 decoupled from the bedrock and therefore its data could not be trusted. Coseismic tilt jumps of -63.9 and 126.3 μradian were recorded by T1(y) and T1(x), respectively. T1(x) recorded significant aftertilt, a phenomenon not previously observed with in-mine seismic events (Spottiswoode and Milev[2006]).

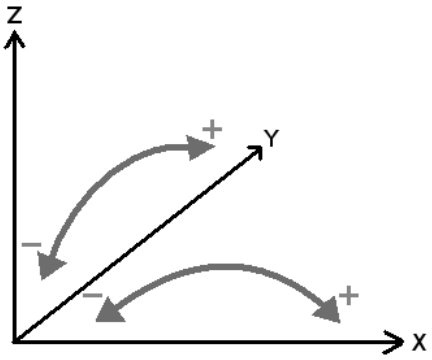

Figure 3. Rotational motions that lead to positive and negative tilt measurements in both x and y components of the installed tiltmeters

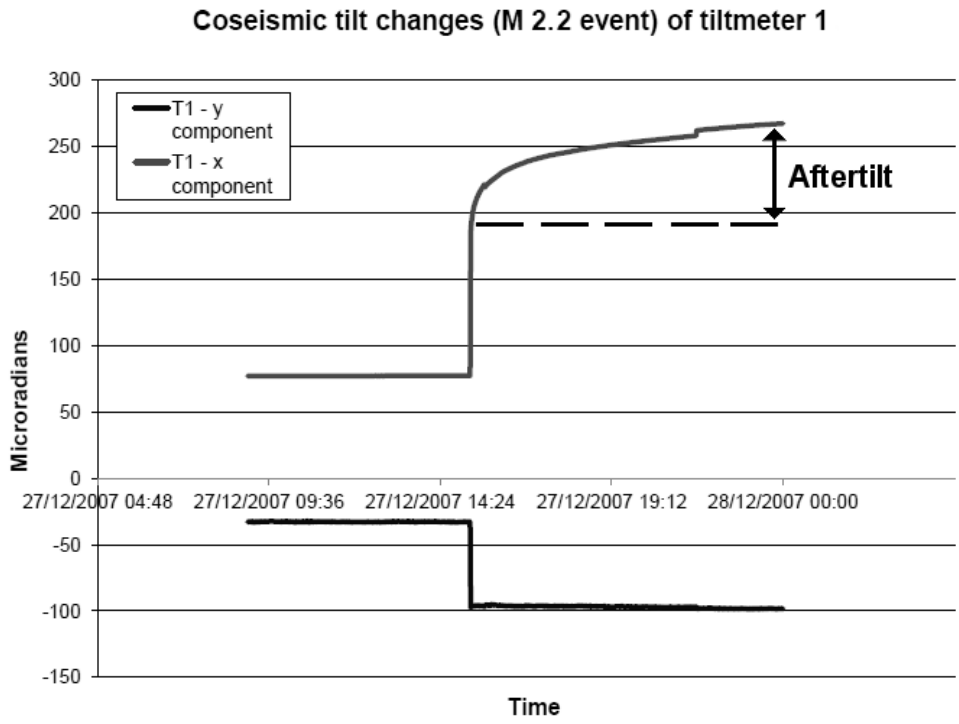

Figure 4. Tilt changes associated with the *M* 2.2 event recorded by the x- and y-components of tiltmeter 1

SEISMIC ANALYSIS OF THE M 2.2 EVENT

The *M* 2.2 event located less than 50 m away from site. Together with the tiltmeter, the event was also successfully recorded by the AE network. The mainshock of the *M* 2.2 event, as determined by the in-mine seismic network, lies within the dyke, and 60% of the more than 20 000 aftershocks, located with the AE network (Yabe *et al.*[2009] and Naoi *et al.*[2011]), that are associated with the main rupture are also situated within the dyke (Figure 5). This is in contrast to what is intuitively expected, where in-mine rupture or failure generally occurs along structural weaknesses, such as a dyke-quartzite (host rock) boundary. The rupture and faulting within the dyke was normal and according to the aftershock distribution the rupture plane had a dip angle of ~60° in compliance with the Coulomb failure criterion (Yabe *et al.*[2009]). After inversion of the in-mine seismic data, one of the nodal planes of the Centroid Moment Tensor was found to dip at 56°, which is very similar to the orientation of the aftershock cluster (Naoi *et al.*[2011]). The aftershock distribution shows the rupture plane to be approximately 4 m in thickness and 100×80 m^2 in areal extent. The aftershock extent compares well with the calculated rupture radius of r = 75 m (Naoi *et al.*[2011]), if the circular crack model of Sato and Hirasawa[1973] is assumed, and the corner frequency of 15 Hz calculated for the mainshock (Naoi *et al.*[2011]) is used. Analysis of the individual waveforms of the event by Naoi *et al.*[2011] produced a seismic moment of 2.9×10^{12} N·m. In contrast, calculations using the same data by the Institute of Mining Seismology (IMS, Hofmann[2012], pers. comm.) gave a seismic moment of 9.875×10^{11} N·m, a corner frequency of 24.7 Hz and a source diameter of 110 m (Brune model, Brune[1970]) (Hofmann *et al.*[2012]). Initial rupturing along the plane, as determined by the mine's network, took place approximately 30 m above the tunnel and cubby (Figure 5). However, owing to the spatial distribution of the in-mine seismic network and the fact that S-waves could not be picked from the AE network, the location of the initial rupture (especially in the vertical direction) has large uncertainty (~20 m). The same rupture point (Figure 5) was obtained when locations of aftershocks that have a pattern of P-wave arrival times similar to that of the mainshock were considered representative of the location of the mainshock.

MODELLING TOOLS

Two modelling tools were used to try to reproduce the recorded tilt, one an analytical tool and the other a numerical package. The analytical tool consists of two formulae by which the horizontal tilt (in two orthogonal directions), due to a single displacement on a rectangular plane, is calculated. The formulae form part of an entire set of closed three-dimensional (3D) analytical expressions that are used to compute the internal displacements and strains due to shear and tensile faults for both point and finite rectangular sources (Okada[1992]). Numerical calculations of the displacement field due to slip on a plane (from which tilt is derived) are done by means of a code, called DIGS (Discontinuity Interaction and Growth Simulation, Napier[1991], Napier and Hildyard[1992]).

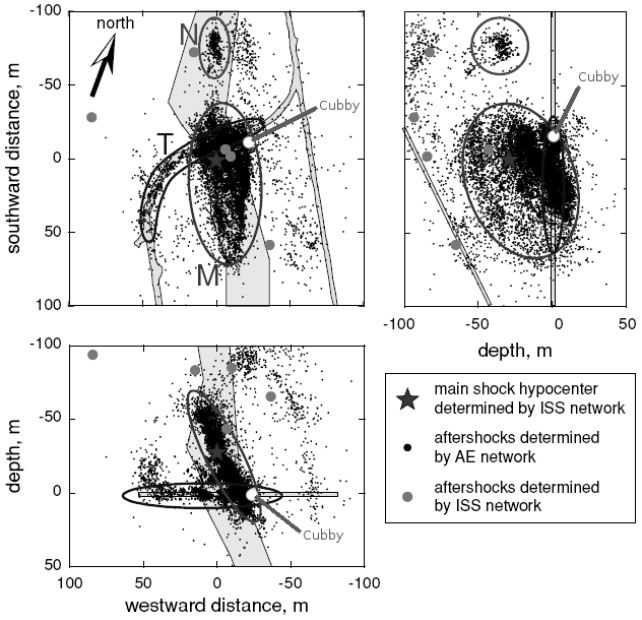

Figure 5. The more than 20 000 aftershocks determined with the AE network. Encircled are the aftershocks associated with the *M* 2.2 rupture plane and the location of the initial rupture (mainshock). Also shown is the location of the cubby containing the tiltmeters (modified from Yabe *et al.*[2009])

In contrast to the 3D analytical tool used, DIGS is two-dimensional (2D), however, the number of slip parameters on the rupture plane that are user-definable far exceeds the two that can be varied in the analytical case, namely, the size of the rectangular source and the average slip. The use of a 2D code, apart from providing appropriate first order approximations of tilt, is in one way justified owing to one component of tiltmeter 1 (T1(x)) being approximately perpendicular (within 5° to 10°) to the strike of the rupture plane (compare Figures 2 and 5). Both analytical and numerical tools compute stress and strain variations in the rockmass with the assumption that it behaves perfectly elastically (Okada[1992] and Napier[1991]).

Previously, the Map3D modelling package (Wiles[2010]), was used to reproduce the actual *M* 2.2 rupture and displacement while taking into account factors such as stress state and the presence of excavations and tunnels (Hofmann *et al.*[2012]). Results of the study, were used as input to the current study, where the average shear stress on the rupture plane = 31.98 MPa, average normal stress on the fault plane = 53.80 MPa, peak internal frictional angle before and after rupture of 25° and 28.5°, respectively, and a peak cohesion of 12.20 MPa. The residual cohesion after fracturing was assumed to be zero.

According to the aftershock distribution as determined by the AE network (Figure 5), most of the rupture took place inside the PG dyke; therefore, the elastic properties of the dyke dictated the amount of slip on the rupture plane. A transmission test based on the seismic velocities of the dyke was completed (Naoi *et al.*[2008]), and a Young's Modulus of 100 GPa and Poisson's ratio of 0.26 was obtained. Using one of the classical equations of elasticity:

$$G = \frac{E}{2(1+v)}, \quad (1)$$

where G is the shear modulus (GPa), E is Young's Modulus (GPa) and v is Poisson's ratio (unitless), the shear modulus of the dyke was calculated to be 40 GPa. Further calculations, using the equation:

$$M_0 = GAD, \quad (2)$$

where M_0 is the seismic moment of the event (N·m) and A the area of rupture (100×80 m^2), produced an average displacement (D) of 3 mm for the IMS determined seismic moment, and 9 mm for the value determined by Naoi *et al.*[2011]. The product of A and D is known as the source potency, P.

RESULTS

The aim of modelling in the current study is to use the analytical and numerical tools and input variables available to reproduce and interpret the recorded tilt. From such a comparison clarity will be gained on which faulting parameters mostly influence tilt, and, thereafter, further constraints can be placed on the input parameters used during modelling.

3D Modelling

Approximating the rupture area as a plane, and, assuming it has a constant dip of 60°, results in a modelling set-up where tiltmeter 1 locates 53 m down the plane, 70 m across it and 16 m horizontally away from it along the tunnel (Figure 6).

Modelling started with the analytical formulae of Okada[1992] and using the configuration in Figure 6 with the y-component perpendicular and x-component parallel to strike. Allowing the entire rupture plane to slip 9 mm (as calculated with the seismic moment from Naoi *et al.*[2011]) and at once (infinite rupture velocity), and, selecting the Young's modulus (E) and Poisson's ratio (v) stated in the previous section, results in T_{zx} = 5 μradian (horizontal tilt in the x-direction) and T_{zy} = 111 μradian (horizontal tilt in the y-direction). Varying E from 70 to 110 GPa results in no change in the latter tilt values. However, varying v from 0.2 to 0.3, changes T_{zx} from 5.28 to 5.18 μradian, and, T_{zy} from 109 to 113 μradian. By far the greatest variation in calculated tilt is observed when varying the amount of slip. A doubling in D results in a doubling of both T_{zx} and T_{zy}, in the same way, when D is halved, T_{zx} and T_{zy} are halved as well.

By dividing the rupture plane into 1 m^2 squares and sequentially allowing each piece to slip at a time, an indication is obtained of how each element contributes to tilt at T1. Also, with such a test, the effect of the location of a tiltmeter relative to a point of rupture is observed. In Figure 7 the tilt contribution of each piece (with 9 mm of slip on each square) to T_{zx}(a) and T_{zy}(b), at the location in Figure 6, is shown.

Studying the results thus far, it can be concluded that the factors that influence the amount of tilt most, are the amount of displacement along the rupture plane and the relative distance between the 1 m^2 block rupturing and the observation point. The latter factor is observed in Figure 7, and, is also anticipated owing to the rapid fall off of tilt energy with distance when compared to decreasing seismic energy with distance (Spottiswoode and Milev[2006]). Also, tilt along strike (T_{zx}) is as much as 2 orders of magnitude less than tilt perpendicular to strike (T_{zy}).

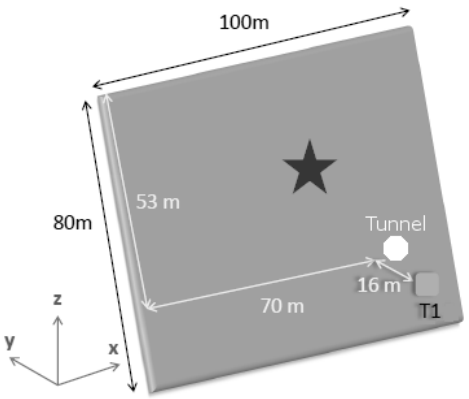

Figure 6. The entire plane of fracture containing the initial rupture point (star). Also shown is the location of tiltmeter 1 relative to the plane

Modelling in DIGS

Starting with E = 100 GPa, v = 0.26 and an average displacement of 9 mm along the rupture, the same process was repeated in DIGS. The value of T_{zy} (T_{zx} cannot be computed due to DIGS being a 2D tool) deduced from the displacement field with D = 9 mm is 103 μradian. Again, varying E has no effect whilst changing v from 0.2 to 0.3 results in T_{zy} changing from 101 to 105 μradian. Also, doubling and halving D has the same effect as in the case of 3D modelling. Plotted in Figure 8, are the resultant tilt contributions of each 1 m segment of the 2D rupture, each displaced by 9 mm, compared with a tilt profile extracted from Figure 7b at 70 m along strike. Encouragingly, and overall, the preliminary values of T_{zy} calculated with analytical and numerical tools, and their position-dependent behaviour, are comparable. However, rupturing with infinite velocity is unlikely, as attested by unequal values of

modelling and data from T1 (x and y) (Figure 4, on the basis that one component of the tiltmeter is approximately perpendicular to the strike of the fracture plane). Therefore, further testing is needed.

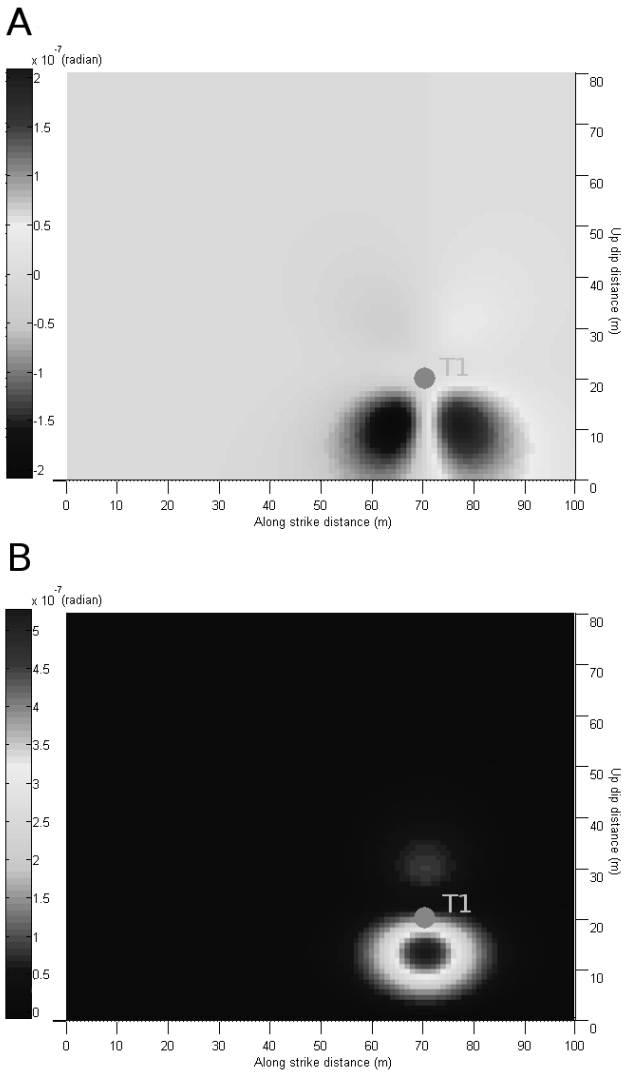

Figure 7. The 100 × 80 m^2 rupture plane, divided into 1 m^2 blocks, and, the contribution of each block to the total tilt T_{zx}(A) and T_{zy}(B), when displaced by 9 mm. The projection of the observation point (T1) onto the plane is indicated

Extended Source Model

Rupturing that starts at a single point and distributes in a systematic or arbitrary manner to the rest of the final source plane is more realistic. Of the two tools used thus far, modelling where the amount of displacement varies along the rupture plane can only be achieved in DIGS, so, hereinafter, only modelling results from DIGS will be presented.

To allow the source potency $(P = AD)$ to remain equal for the single rupture point scenario, and the case where rupture occurs instantaneously all along the source plane, the displacement at that initial rupture point has to be larger than 9 mm. To determine the said initial displacement value, modelling was constructed such that the initiation point was located at the location suggested by previous studies (Figures 5 and 6), and the normal and shear stresses applied on the plane and internal friction angle and cohesion of the rupture was equal to the values given in Hofmann *et al.*[2012]. On a trial-and-error basis, a displacement value of 26 mm at the suggested rupture point was determined appropriate for the source potency to remain intact. As the point was moved closer to the edges of the entire rupture, the value of 26 mm had to be increased by 1–2 mm to retain the needed source potency. With an initial displacement of 26 mm, and the displacement decreasing away from this point to zero at the edges, T_{zy} at the measurement location is 81 μradian, therefore, too low. The value of T_{zy} can be increased (to fit actual observations) by, for instance, decreasing the shear stress or increasing the normal stress, which will both necessitate the increase of the initial displacement, and, in turn, increase tilt. However, the amounts of stress, internal friction angles and cohesion values were very accurately determined by an independent modelling process and taking into account many relevant factors, and are therefore trusted. Even when admitting an error in the input variables of a few percent, the calculated tilt will still remain too low when compared to observations.

As previously determined, the two main variables contributing to tilt, are, the displacement on the rupture plane, and, the position of the observation point relative to the plane or the initial point of rupture (Figures 7 and 8). As stated, the amount of displacement, even when allowing error in other input variables, is fixed. Therefore, the only variable left, that if altered will have a significant effect on tilt, is the location of the rupture point. If Figure 8 is interpreted not as the contribution of each rupturing section to the total tilt, but, rather as a measure of the location-dependent sensitivity of rupturing to the total tilt, then, it is clear that if rupture starts (or only occurs) from 5 to 40 m up dip (especially in between 6 and 20 m), the measured tilt will be much larger than if rupturing started elsewhere. The proposed initial rupture point is located at approximately 47 m up dip, which is outside the highly sensitive region, thus, to achieve the desired measured tilt during modelling, this points needs to be shifted lower down the rupture plane. When rupturing starts at 26 m up dip, the resultant tilt is comparable to the measured value for T_{zy}, namely, 126.3 μradian (T1(x)).

Another possibility, in which both the suggested (47 m up dip) and recently calculated (26 m up dip) rupture points are included, is a continuous segment, from the one point to the other, that as a whole initiated rupturing. Owing to the increase in length, and in an attempt to retain source potency, the displacement value on the said segment equated to 14 mm. The tilt associated with the 21 m long segment, with D = 14 mm, is 106 μradian, which is too small when correlated with T1(x).

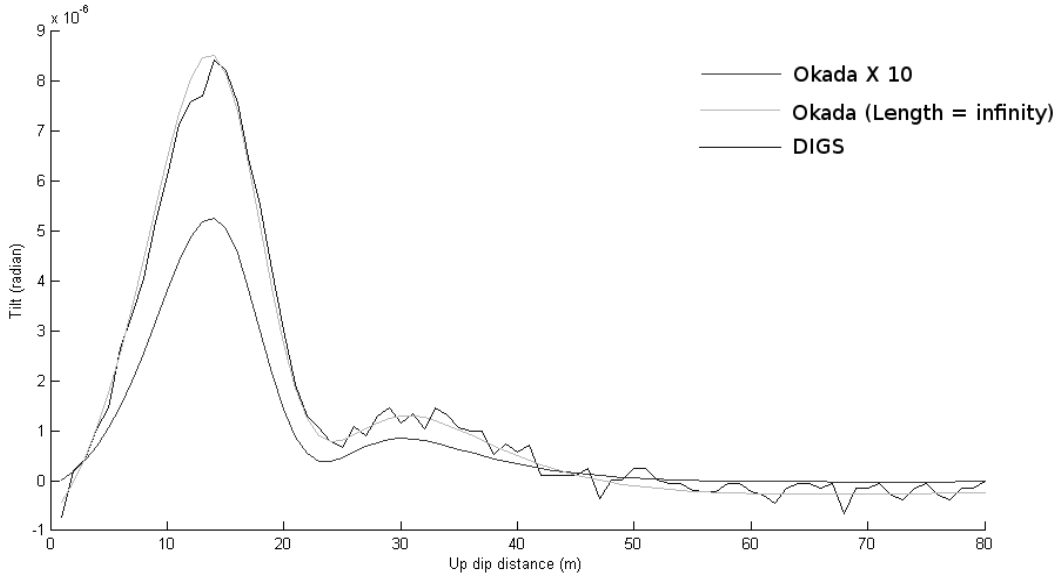

Figure 8. Contributions of each 1 m segment of the 2D rupture to the total tilt T_{zy}, calculated with DIGS. Also shown, for comparison, are sections, one extracted from Figure 7b at 70 m along strike (increased by an order of magnitude), and the other extracted from the same result but when the length of the fault is set to 200 km

Using the average displacement of 3 mm across the rupture plane, as determined using the IMS's seismic moment, a tilt value of 34 μradian (a third of the value calculated with $D = 9$ mm) is obtained. Repeating the same process here, if a single rupture point is assumed, then the displacement at this point has to be 4 mm in order to keep the source potency at a constant value. However, no calculated tilt value approaches the real measurement, irrespective of how the rupture point is shifted around. A maximum value of only 42 μradian is achieved, and this occurs when the initial rupture point is at 14 m up dip.

DISCUSSION AND CONCLUSIONS

During the analyses of data, and due to one component of tiltmeter 1 aligning approximately perpendicularly to the strike of the rupture plane, much of the focus has been placed on only correlating modelled results of the perpendicular component (T_{zy}) with real data measured in that direction, namely, T1(x). However, in contrast to modelling results, the measured component parallel to strike, T1(y), is not small compared to its orthogonal equivalent. For tiltmeter T1, the coseismic tilt jump in the y-component is only a fraction smaller than the jump measured in the x-component (not two orders of magnitude smaller, as was shown during modelling), therefore, the tilt vector points in a direction somewhere in between x and y, and, the vector's magnitude is larger than both 126.3 μradian (T1(x)) and 63.9 μradian (T1(y)). By simple vector addition the maximum value of tilt (T1) is calculated to be ~142 μradian and it points in a direction 30° from the +x axis, measured clockwise. This raises questions about the assumed simplicity of the source (Figure 6).

From the modelling results it was deduced that the initial rupture point had to be closer to the tiltmeter locations. However, a larger tilt could also have been obtained by moving the entire rupture plane closer to the tiltmeter locations, whilst the location of the initial rupture remains unchanged (in other words, decreasing the horizontal distance of 16 m in Figure 6). Indeed, the rupture plane, as determined by AE network, is, in fact, a slab rather than a plane, a slab with thickness 4 m. During modelling, the centre of this slab was taken as the plane of rupture, therefore, realistically; the true rupture plane could have been located closer to the tiltmeters. And, because of the high location-dependency of tilt magnitude, a closer plane would have resulted in an increase in tilt. It should be noted though, that, in order to achieve the recently calculated larger tilt value (~142 μradian) during modelling, the rupture point would still have to be shifted closer, even if the actual rupture plane was assumed to be nearer to the tiltmeters. Thus, the researchers conclude, with certainty, that initial rupturing occurred closer than what was previously suggested (Naoi *et al.*[2011]), but still within the error (~20 m) of that earlier calculation. To obtain even greater clarity on how close the rupture point was, future modelling needs to include structures such as the surrounding tunnels.

Determining the reasons for the initial rupture point locating lower down the final rupture plane (or for that matter in the location where it was originally calculated to be) is beyond the scope of the current topic (and the resolving abilities of the data), but, it is still an important research aim. 3D stress and strain modelling of the source (that is more complex than the plane suggested in the current study), and regions surrounding it, is a recommended research topic. However, this modelling needs to be done in conjunction with the acquisition and analyses of more good quality data.

Not much attention has been given to the noticeable aftertilt observed in T1(x) (Figure 4). The cause of aftertilt is still unclear, but it is usually considered a result of either coseismic or aseismic expansion of the seismogenic zone (rupture plane), or, coseismic or aseismic activity within the original seismogenic zone, which follows the main event (manifests as a jump in tilt data). If the seismogenic zone expanded coseismically or aseismically, and, taking into account the amount of aftertilt recorded in T1(x) (~70 μradian), it is most probable that it expanded to the bottom and bottom right of the seismogenic zone. The sensitivity of tilt to any other boundary of the zone is too low to result in the desired amount of aftertilt (Figures 7). Another possibility is activity occurring within the identified zone after the main event, especially in the bottom right corner of the zone where a dense collection of aftershocks are present (Figure 5).

ACKNOWLEDGEMENTS

The authors of this paper would like to express their thanks to the SATREPS project "Observational studies to mitigate seismic risks in mines" funded by JST-JICA Science and Technology Research Partnership for Sustainable Development for their financial support and encouragement. We wish to express our sincere appreciation to the rock engineering staff of Mponeng gold mine for their assistance and cooperation.

REFERENCES

BRUNE, J.N. Tectonic stress and the spectra of seismic shear waves from earthquakes, *J. Geophys. Res.*, vol. 75(26), 1970. pp. 4997–5009.

HOFMANN, G., OGASAWARA, H., KATSURA, T. and ROBERTS, D. An attempt to constrain the stress and strength of a dyke that accommodated a M_L 2.1 seismic event, in *Proc. 2nd South. Hemisphere Int. Rock Mech. Symp. (SHIRMS)*, Sun City, South Africa, 2012. p. 15.

McGARR, A. and GREEN, R.W.E. Measurement of tilt in a deep-level Gold Mine and its relationship to mining and seismicity, *Geophys. J. R. astr. Soc*., vol. 43, 1975. pp. 327–345.

NAOI, M., NAKATANI, M., YABE, Y., PHILIPP, J. and JAGUARS-group. Very high frequency AE (< 200 kHz) and micro seismicity observation in a deep South African gold mine – Evaluation of the acoustic properties of the site by in-situ transmission test, *Seism. Res. Lett.*, vol. 79(2), 2008. p. 330.

NAOI, M., NAKATANI, M., YABE, Y., KWIATEK, G., IGARASHI, T. and PLENKERS, K. Twenty thousand aftershocks of a very small (M 2) earthquake and their relation to the mainshock rupture and geological structures, *Bull. Seism. Soc. Am.*, vol. 101(5), 2011. pp. 2399–2407.

NAPIER, J.A.L. Energy changes in a rockmass containing multiple discontinuities. *J. S. Afr. Inst. Min. Metall.*, vol. 91(5), 1991. pp. 145–157.

NAPIER, J.A.L. and HILDYARD, M.W. Simulation of fracture growth around openings in highly stressed, brittle rock, *J. S. Afr. Inst. Min. Metall.*, vol. 92(6), 1992. pp. 159–168.

OGASAWARA, H., DURRHEIM, R.J., NAKATANI, M., YABE, Y., MILEV, A., CICHOWICZ, A., KAWAKATA, H., MORIYA, H. and JST-JICA SA research group. A Japanese – South African collaboration to mitigate seismic risks in deep gold mines, in *Proc. 1st Hard Rock Safe Safety Conf.* (ed. van der Westhuizen, J.), Southern African Institute of Mining and Metallurgy, Johannesburg, 2009. pp. 115–134.

OKADA, Y. Internal deformation due to shear and tensile faults in a half-space, *Bull. Seism. Soc. Am.*, vol. 82(2), 1992. pp. 1018–1040.

SATO, T. and HIRASAWA, T. Body wave spectra from propagating shear cracks, *J. Phys. Earth.*, vol. 21, 1973. pp. 415–431.

SPOTTISWOODE, S.M. and MILEV, A.M. A study of mine stability using records of ground tilting, in *Proc. of the 41st U.S. Rock Mech. Symp.*, Golden, Colorado, 2006. CD-ROM, Paper No. 06-1168.

WILES, T. *Map3D User's Manual*, Mine Modelling Pty Ltd (www.map3d.com), Australia, 2010.

YABE, Y., PHILIPP, J., NAKATANI, M., MOREMA, G., NAOI, M., KAWAKATA, H., IGARASHI, T., DRESEN, G., OGASAWARA, H. and JAGUARS-Group. Observation of numerous aftershocks of an M_w 1.9 earthquake with an AE network installed in a deep gold mine in South Africa, *Earth Planets Space*, vol. 61, 2009. pp. e39–e52.